EXPERIMENTAL INVESTIGATION AND THERMAL ANALYSIS OF COUPLER-ROCKER BALL BEARING

Abdullah JAMIL [*1], Masri Bin BAHAROM[1], Tamiru Alemu LEMMA[1], Tadimalla Varaha Venkata Lakshmi Narasimha RAO

[*1]Department of Mechanical Engineering, Universiti Teknologi PETRONAS, 32610 Bandar Seri Iskandar, Perak, Malaysia

[2]Department of Mechanical Engineering, SRM Institute of Science and Technology, Kattankulathur – 603203, India

[*]Corresponding author; E-mail: iabdullahjamil@yahoo.com

Ball bearings are widely used in many machineries and industrial applications. Thermal behaviour of oscillating ball bearings is unknown due to its complex pendulum-like motion and is discussed in this research. In this research, the effect of operating conditions of the oscillating bearing performing coupler-rocker motion on the heat generation is experimentally investigated and verified using mathematical model. For this purpose, a coupler-rocker bearing testing rig was designed and fabricated and the test bearing is splash-lubricated in an oil sump. The loading of test bearing was done using two extension springs. The applied load on the bearing was varied from 0 to 750 N while the crank rpm was varied from 1200 rpm to 1800 rpm. Three lubricant grades were used namely, SAE30, SAE40 and SAE50. Experimental results showed that the temperature of coupler-rocker bearing approaches steady-state at about 12 minutes for all cases. The steady-state temperatures at variable conditions are observed to follow a linear trend.

Key words*: Thermal analysis; Oscillating bearing; Experimental testing; Ball bearing; Four-bar mechanism; Coupler-Rocker*

1. Introduction

There are many industrial machineries and robots which use rolling element bearings at moving pairs of linkage joints. The lubrication done on these bearings include grease or forced oil lubrication through internal passages. These joints include bearing performing full rotation as well as oscillating motion. One such example of full rotation bearing is the conrod – crankshaft joint while the bearing performing oscillating motion can be found in the coupler and rocker joint in a four-bar mechanism.

Salah *et al*. [1] designed and fabricated a novel Crank-Rocker IC Engine which works on the principle of four-bar mechanism. The engine uses a coupler-rocker joint where a ball bearing is used as a pin joint. Oil sump is used for the splash lubrication of its crank-coupler and coupler-rocker bearings. The overall performance of the coupler-rocker bearings under splash lubrication is unknown because no reported literature can be found. It is questionable whether the coupler-rocker bearing

thermally behaves the same as the fully-rotating ball bearing. Hence, designers and engineers need to study the thermal behaviour of oscillating bearing in order to optimize the Crank-Rocker Engine.

There are many significant parameters that affect the bearing temperature, such as the rotational speed and applied load on the bearing, the lubricant viscosity etc. Many researchers have performed thermal analysis of journal and rolling bearings performing complete rotation under different operating condition [2–10].

Choi and Lee [3] calculated the heat generation within the ball bearing and used this generated heat to analyse the temperature variation in the bearing using FEA. They compared the data from ANSYS with experimental results and found out that it was a good approach but not accurate. Babu and Dhamotharan [11] performed a simulation of temperature distribution of CNC lathe assembly. They calculated the bearing heat generation and incorporated that in ANSYS® simulation and run the analysis in Transient Thermal module. Qi *et al*. [12] compared the calculated total thermal resistance from the mathematical model with the thermal resistance obtained from FEA of the bearing. They concluded that the thermal resistance network can be used to describe the temperature variation within the bearing.

The generated heat in the ball bearings has been calculated by many researchers [5, 6, 11, 13, 14] using a set of equations. The variables used in the calculations depend upon the bearing and lubricant used. Their values can be acquired from data sheets from respective distributors. Some authors [2, 3] incorporated frictional moment due to gyroscopic and spinning motion of balls at contact area when calculating heat generation in axially loaded angular-contact ball-bearings. This spinning torque is not present in deep-groove ball-bearings as the contact angle between balls and raceways is 0°. Therefore, there is no slip motion of balls in deep-groove ball-bearings.

The heat generated in the bearing is dissipated to the surrounding through modes of heat transfer. Most researchers [5, 6, 8, 12, 15–18] designed thermal resistance network model to calculate the heat transfer through conduction and convection from the bearing. This method comprises of the network of resistances constructed among different components of the test bearing assembly. These components i.e. nodes, include inner and outer races, balls, shaft, ambient air, lubricating oil and bearing housing, etc. Radiation is ignored in the current study due to low surface-temperatures. Harris [19] presented a set of expressions to calculate the heat transfer from bearing through conduction and convection.

The current study is intended at producing a universal model applicable to several applications related to oscillating bearings. Jamil *et al*. [20] proposed an advanced model and simulation to study the thermal behaviour of oscillating ball bearings. The procedure described in the current study is open to rolling element bearings of various sizes and the proposed model is adopted to predict the thermal behaviour of bearing components. Useful equations and operating conditions are mentioned to predict the values of the parameters for deep-groove ball-bearing with splash lubrication when radial load is applied on it. For validation of the mathematical model, experiments were performed on a custom designed and fabricated bearing testing rig for different angular speed, external radial loads and lubricant viscosity grade.

2. Test Rig Assembly

2.1. Description of Apparatus

A testing rig was designed and fabricated to test the thermal behaviour of an oscillating ball bearing. The rig consists of four-bar mechanism with its crank link connected to the crankshaft of the driver engine and the bearing testing rig is shown in fig. 1. The link parts are made of AISI 1050 Carbon Steel. The rig is designed to test SKF 61902 Deep Groove Ball Bearing as a coupler-rocker joint. The inner and outer diameters of the bearing are 15mm and 28mm respectively. The rig is capable of testing the bearing at crank speed up to 2000 rpm.

The driver engine crankshaft speed could be adjusted independently by the throttle inlet valve screw position and measured using tachometer. The crankshaft of the driver engine is connected to the crank link of the testing rig using flange. To protect the shafts and rig from deflecting, a ball bearing (SKF SY 25 TF) Plummer block is installed. The oscillating coupler-rocker bearing is splash lubricated in 1 litre lubricant oil in the tank. The test bearing is half dipped in the lubricant in tank when the rocker is at the extreme top position. Only the test bearing and lower coupler part is in contact with the lubricant oil. The complete testing rig assembly and coupler-rocker test bearing is shown in fig. 2(a-b). A slit was made in the rocker link to firmly place thermocouple wire in rocker link and to make direct contact of thermocouple tip with the outer ring surface of the test ball bearing.

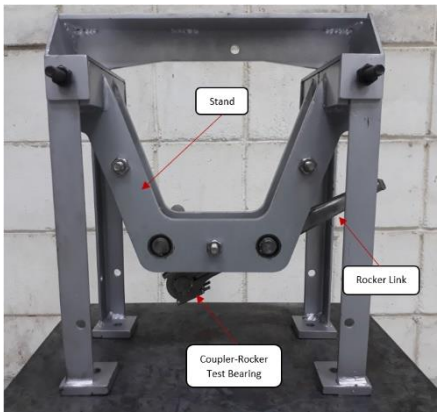

Figure 1. Coupler-Rocker bearing testing rig

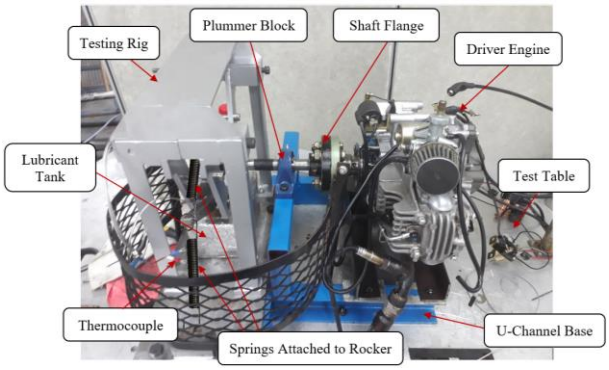

Figure 2(a). Coupler-Rocker bearing testing rig assembly

Figure 2(b). Thermocouple connection to the outer ring of the Coupler-Rocker test bearing

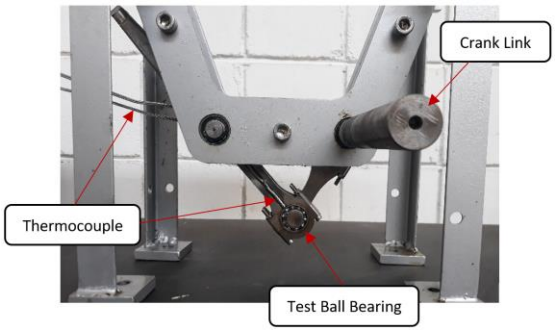

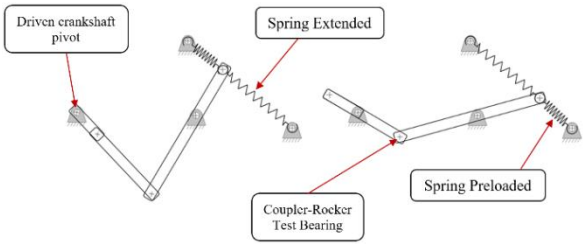

Figure 3. Schematic of springs attachment at rocker link

The loading on the oscillating bearing is applied indirectly using the rocker link. Two extension springs were attached to the rocker link at its

tip on opposite sides. As one spring extends, the other retracts and vice versa as shown in fig. 3. According to Hooke's Law for linear extension springs, the restoring force within the spring is directly proportional to its extension as given in eq. (1):

$$F_1 = -rx_1 \; ; \qquad F_2 = -rx_2 \tag{1}$$

where F_1 and F_2 are the loads being applied on the rocker link from two extension springs and r is the spring rate. The negative sign represents the opposing restoring force.

The forces exerted by the two springs is shown in fig. 4. The resultant of these two extension spring forces is given by $F = F_1 + F_2$ and the resultant was found to have a constant load on the rocker link which is radially applied to the test bearing.

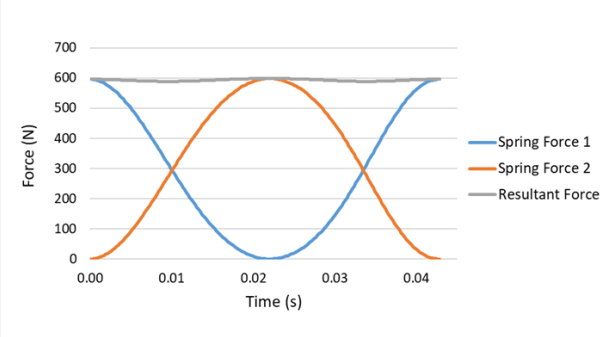

Figure 4. Variation of 11.8N/mm springs restoring force and their resultant on rocker links at 1400rpm crank speed

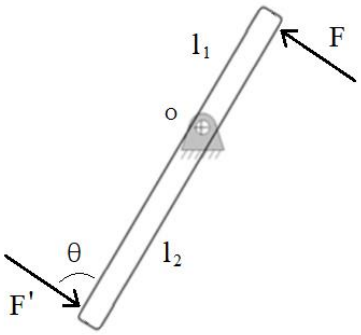

Figure 5. FBD of rocker link load transfer

Fig. 5 shows the free body diagram (FBD) of the rocker link illustrating the transfer of load from the rocker upper end to the coupler-rocker bearing at the other end. By taking the moment about pivot O of the rocker link, the dynamic equilibrium equation for the rocker link is given below:

$$+\circlearrowleft \Sigma M_o = I\alpha \tag{2}$$

$$F * l_1 + F' * Sin\theta * l_2 = I\alpha \tag{3}$$

$$F' = \frac{I\alpha - F * l_1}{Sin\theta * l_2} \tag{4}$$

Eq. (4) shows the formula for the magnitude of load transferred to the coupler-rocker bearing. This magnitude of bearing force is variable and therefore, an arithmetic average is taken in the calculation.

2.2. Instrumentation

The test rig is equipped with thermocouples and tachometer to measure the bearing temperature readings and crank angular speed. A K-type thermocouple is attached on the outer surface of the ball bearing and another thermocouple is dipped inside the oil-sump to measure the oil temperature. It is to be noted that ball bearing temperature is of interest and the temperature of the oil in sump is only for validation purposes. The K-type thermocouple probe was connected to the NI-9211 C-Series

Temperature Module in the Analogue Input (AI0). This module was inserted in the Compact RIO (cRIO) Controller Chassis (NI-cRIO 9063). The data was recorded from thermocouple to cRIO which was transferred to PC through Ethernet LAN cable. A graphical code was developed in National Instruments™ software LabVIEW™ which was used to communicate with the NI hardware.

3. Modelling and Simulation

The overall frictional heat generation in the ball bearing can be investigated thoroughly by considering the factors like bearing type, external load, lubrication type, rotational speed, geometry of objects etc. Afterwards, the heat transfer processes are analysed which includes conduction within the components of the bearing and linkages along with the convection to the surroundings. Once the bearing system components temperature distribution is calculated using initial conditions, the new oil viscosity is calculated to renew the heat generation rate. This step is repeated iteratively until the steady-state condition for temperature is achieved. It is noted that heat transfer through radiation is ignored due to low surface-temperatures in the study. The block diagram of the bearing model is shown in fig. 6.

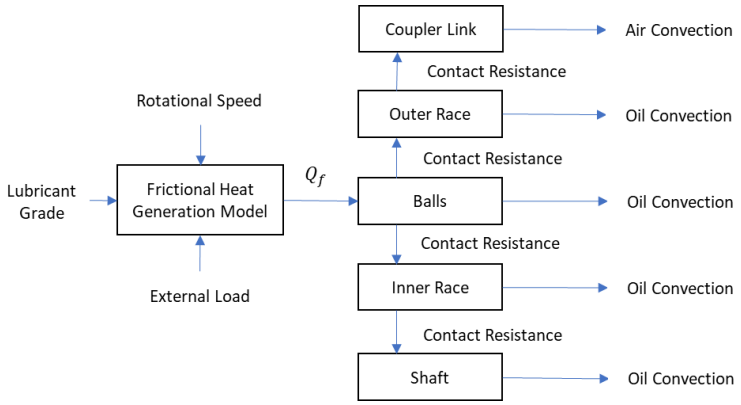

Figure 6. Block Diagram of the bearing model

3.1. Frictional Heat Generation Model

The overall power loss in the bearing due to the frictional contact between the bearing surfaces and the viscous drag is called the total frictional torque. The frictional torque is challenging to be estimated to the variance of multiple factors such as, frictional coefficient estimation between the bearing surfaces and the change in viscosity of lubricant with temperature. A mathematical formulation described by Khonsari and Takabi [5] in their research for the thermal analysis of simple fully-rotating ball bearing is adopted in this study. It is assumed that the behaviour of a coupler-rocker bearing is the same as that of a fully-rotating ball bearing, and the validity of this assumption is determined from the experimental results.

The total frictional torque in the oscillating ball bearing is provided by Stein and Tu [21]:

$$M = M_v + M_l + M_f \tag{5}$$

where $M_{v,}$ M_l and M_f are the frictional torques due to the viscous drag, applied load and due to flange angles. Since ball bearings do not have flanges, therefore the torque due to flanges is ignored in

this case. The formula for individual frictional torques were acquired from Harris [19] as shown below:

$$M_l = f_1 F_\beta d_m \tag{6}$$

$$M_v = 10^{-7} f_o (v_o n)^{\frac{2}{3}} {d_m}^3 \tag{7}$$

where f_1 is the factor depending upon bearing design and relative load, F_β is the factor depending upon the magnitude and direction of the applied load, d_m be the mean diameter of bearing, f_o is the factor depending upon type of bearing and method of lubrication, v_o is the kinematic viscosity of lubricant, n is the bearing rotational speed in rpm. Since, the coupler-rocker bearing is performing an oscillating motion and its angular speed is continuously varying, the average of angular speed of coupler-rocker bearing is taken. The variable values for lubricant and bearing can be acquired from the lubricant's data sheet and bearing manufacturer's catalogue.

The total frictional heat generation Q_f in the ball bearing is given by:

$$Q_f = \frac{2\pi n}{60} M \tag{8}$$

It is important to be noted that these formulas are valid to be used for normal conditions of the ball bearing and the lubricant oil level should be maintained according to the bearing manufacturer.

3.2. Heat Transfer Model

A resistance network is modelled according to the experimental bearing setup. This network specifies the resistances in conduction and convection from balls to races, shaft, link, air and oil. Fig. 7 shows the thermal resistance network of the test bearing, which consists of 8 thermal nodes for the bearing assembly. The number of nodes used in the thermal network was found to be sufficient for prediction of bearing temperature. Only a quarter of the actual model was used in this study due to the symmetry of the bearing model. In order to have simplified equations, resistances at each node were calculated and their descriptions are given in tab. 1.

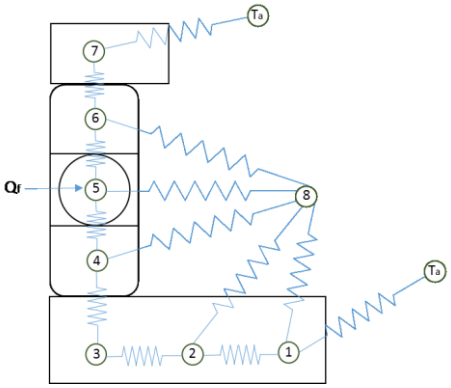

Figure 7. Thermal resistance network of the bearing assembly

Calculated heat generation Q_f was incorporated in node 5 i.e. balls. Each energy balance equation represented the change of heat generation with time at that node. The conductive and convective resistances have the form $R_r = \frac{\ln\left(\frac{R_1}{R_2}\right)}{2\pi kl}$ for radial conduction, $R_a = \frac{\Delta L}{Ak}$ for axial conduction and $R_{conv} = \frac{1}{hA}$ for convection.

Table 1. Description of thermal resistances

Symbol	Description
R_{12}	Axial conduction through the shaft

R_{23}	Axial conduction through the shaft
R_{34}	Radial conduction between inner race and shaft
R_{45}	Radial conduction between balls and inner race
R_{56}	Radial conduction between balls and outer race
R_{67}	Radial conduction between outer race and coupler link
$R_{c,oil}$	Oil convection from races, balls and shaft
$R_{c,air}$	Air convection from shaft and coupler link

where, l, R_1 and R_2 are the width, inner and outer radii of the annular structure respectively, ΔL is the distance between two points, k is the thermal conductivity of material, A is the cross-sectional area through which heat transfers, h is the heat transfer coefficient. For calculating convective resistances, values of respective heat transfer coefficients h needed to be calculated. Reynolds number, Nusselt number, Prandtl number and Grashof number were calculated to find h values. The equations used to calculate heat transfer coefficients for different geometrical objects were proposed by Harris [19].

for rotating ball,

$$\frac{h_v D}{k} = 0.33 Re^{0.5} Pr^{0.4} \tag{9}$$

for cylindrical ring (races)

$$\frac{h_v D}{k} = 0.19(Re^2 + Gr) \tag{10}$$

$$Gr = \frac{Bg(T_s - T_\infty)D^2}{\nu^2} \tag{11}$$

The convection through air are calculated using the following equations:

$$R_{c,air} = \frac{1}{hA} \tag{12}$$

$$\frac{hD}{k} = Nu = 0.119 Re^{\frac{2}{3}} \tag{13}$$

where, D is the diameter of ball, B is the volume expansion coefficient of oil, g is the gravitational constant, T_s is the temperature at surface, T_∞ is the temperature of oil. Low temperature variation has negligible effect on the viscosity of air [22]. Therefore, average viscosity of air was calculated at ambient air temperature and kept constant throughout the calculations. Viscosity of oil, however, varies significantly with temperature and therefore, can be acquired from the lubricant datasheets.

The most used lubricant in the experiments was Castrol Activ 4T 20W-40. The viscosity depends considerably on fluid temperature [23, 24]. Since heat transfer coefficient values depend upon viscosity of oil, therefore, viscosity of oil was varied successively after each iteration. The viscosity-temperature data of 20W-40 oil was taken from lubricant datasheet. Following formulae was generated from the graph using exponential approximation and was used to vary the viscosity of oil in each iteration of mathematical calculations.

$$\nu = 20.94488 + 1573.682\, e^{-0.06958388(T)} \tag{14}$$

where T and ν are the temperature of oil in °C and viscosity of oil in mm^2/s respectively. The viscosity-temperature trend acquired from above mentioned equation is shown in fig. 8. Since the operating temperature of oil throughout the simulation remains above the room temperature, therefore, 20W-40 behaves as SAE40 oil. Same goes for SAE30 and SAE50 grade oils.

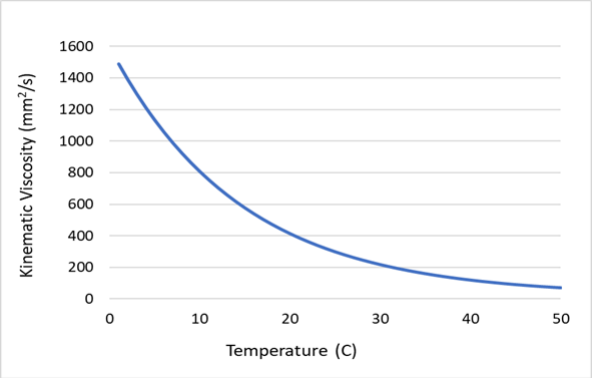

Figure 8. Kinematic viscosity trend of 20W-40 oil with temperature

Considering energy balance equation for each node, one can write a set of 8 partial differential equations with 8 unknown temperatures at each node. Energy balance equations for nodes 4, 5 and 6 with unknown temperature variables are mentioned below:

$$\frac{T_3 - T_4}{R_{34}} + \frac{T_5 - T_4}{R_{45}} + \frac{T_8 - T_4}{R_{c,oil}} = m_3 c_3 \frac{\partial T_4}{\partial t} \tag{15}$$

$$\frac{T_4 - T_5}{R_{45}} + \frac{T_6 - T_5}{R_{56}} + \frac{T_8 - T_5}{R_{c,oil}} + Q_f = m_5 c_5 \frac{\partial T_5}{\partial t} \tag{16}$$

$$\frac{T_5 - T_6}{R_{56}} + \frac{T_7 - T_6}{R_{67}} + \frac{T_8 - T_6}{R_{c,oil}} = m_6 c_6 \frac{\partial T_6}{\partial t} \tag{17}$$

where T is the initial temperature at the node and T' is the temperature at the node after the time step h. Since these are PDEs which needed to be solved at each time step simultaneously, therefore finite difference method was used to solve these energy balance equations iteratively in MATLAB®. The initial temperature of bearing and oil is the ambient temperature of testing rig i.e. 30°C or 303 K.

Once the resistance values were calculated, the energy balance equations were entered in MATLAB® for calculations. Time-step of the iterations was kept very small for relatively accurate results through finite difference method. The code was written in such a way that at each iteration, all the 8 energy balance equations were simultaneously solved for that time step.

4. Experimental Tests

As mentioned in section 2, a testing rig was designed and fabricated to perform experiments on the test ball bearing which is a single-row deep-groove ball bearing (SKF 61902). This bearing is present at the joint of coupler and rocker links and acts as a pin joint which oscillates within 21° range. Due to this oscillating motion, the test bearing is splashed in the oil-sump and is lubricated as well as the generated heat is dissipated. The experiments are performed in a laboratory with environmental temperature of 30°C. The experiments are divided into three categories based on three measurable parameters, namely, applied load, crank angular speed and lubricant viscosity grade. The ranges of the external loads, the crank rotational speeds and the lubricant viscosity grades are given in the tab. 2. The driver engine is started and run at a desired speed. The engine crankshaft takes about 5-10 s to accelerate to reach the required speed which is measured using a digital tachometer. The bearing's

outer ring surface temperature and the oil sump temperatures are measured using K-type thermocouples which are connected to the NI data acquisition chassis and in conjunction with the LabVIEW software. About 15-30 minutes are required to achieve a steady-state condition. Once the bearing temperature is uniform, the driver engine is stopped, and the bearing is allowed to cool down to room temperature for next test.

Table 2. The range of test parameters

External Radial Load (N)	Rotational Speed (rpm)	Lubricant Viscosity Grade
0 N	1200	SAE30
410 N	1400	SAE40
577 N	1600	SAE50
744 N	1800	

5. Results and Discussion

The experimental results are presented and compared with the predicted results of the mathematical model mentioned earlier.

5.1. Verification

A comparative study of results obtained from the experiment and mathematical modelling is done to evaluate the thermal analysis of coupler-rocker ball bearing. The operating conditions of the two models are selected randomly for verification purposes. The first model is the comparison of bearing at 1400 rpm crank speed, 744 N load applied on rocker and the bearing splash lubricated with SAE30 oil. The mathematical calculations are done accordingly and compared with experimental results obtained from the same conditions as shown in fig. 9.

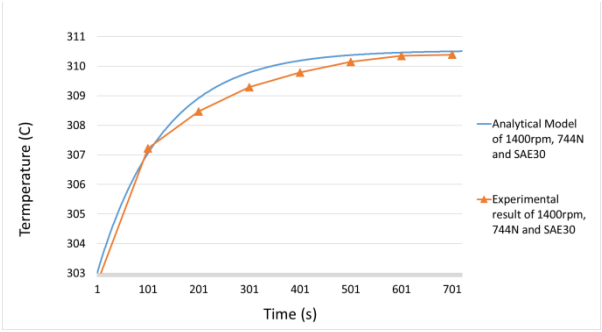

Figure 9. Comparison of experimental and analytical data at 1400 rpm and 744 N load

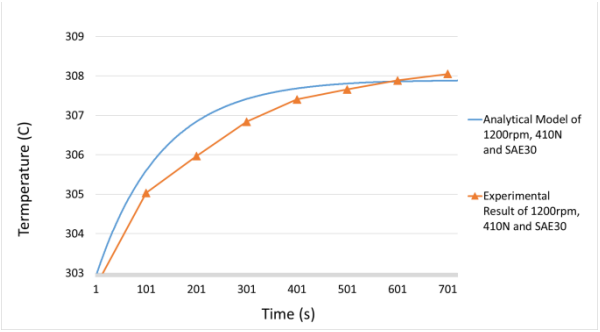

Figure 10. Comparison of experimental and analytical data at 1200 rpm and 410 N load

It is observed that the temperature rises from room temperature rapidly in the beginning then gradually slows down. Eventually, the temperature stabilizes at about 310.5 K. The measured temperature value is slightly smaller in the middle than the calculated value. The reason because of the inaccuracies and uncertainties in the measured values. Heat dissipation to the surrounding

environment from the bearing may resulted in slight drop in temperature reading. The maximum error between the two temperatures data is 0.16%. The second model is the comparison at 1200 rpm crank speed, 410 N load on rocker lubricated with SAE30 oil as shown in fig. 10. It is observed that the temperature rises from room temperature rapidly in the beginning then the rate of change of temperature rise decreases with time. Eventually, the temperature stabilizes at about 306.5 K. The maximum error between the two temperatures data is 0.13%. The maximum difference between temperature readings is 0.4°C. The error is due to the uncertainty in data measurement and heat losses.

5.2. Effects of External Radial Load

The effect of load applied on rocker link on the heat generation rate in the coupler-rocker bearing was investigated. During the experiments, the crank angular speed was kept constant at 1400 rpm while the lubricant grade was kept same i.e. SAE30. Fig. 11 shows the variation in temperature of C-R bearing with time due to the change in applied load.

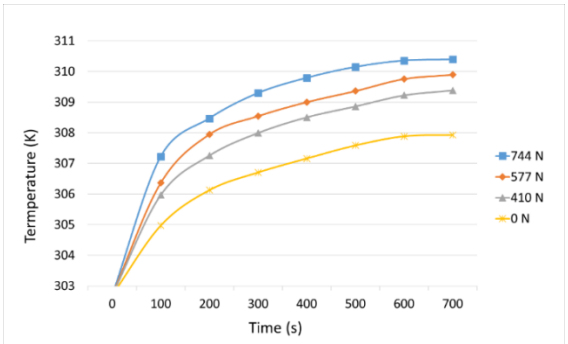

Figure 11. Load variation effect on bearing temperature

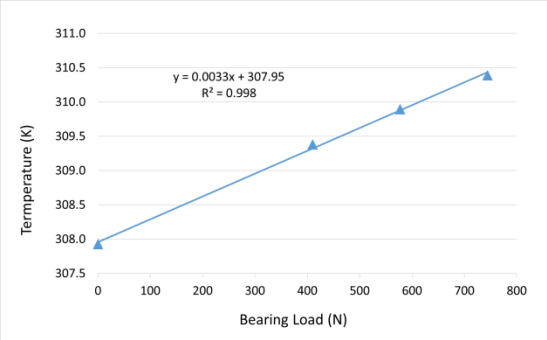

Figure 12. Trend of steady-state temperature with applied load

It is evident that as the load on C-R bearing increases, the frictional moment due to load increases and does the heat generation rate. As a result, the temperature of C-R bearing also rises. The temperature curves rose rapidly in the beginning, but it is reduced gradually with time and the temperature got steady after 650 s or 10.8 min for all the three applied loads. The steady-state temperatures of the bearing having loads of 744 N, 577 N, 410 N and 0 N were about 310.5 K, 310 K, 309.4 K and 308 K respectively. The trend of steady-state temperature values versus load applied on the bearing is shown in fig. 12. It is observed that the trend is almost linear. Hence, it can be said that the steady-state temperature of the oscillating ball bearing rises linearly with the increase in applied load. The Coefficient of Determination (R^2) for the linear curve fit was found to be 0.998.

5.3. Effects of Rotational Speed

The effect of angular speed applied on crank link on the heat generation rate in the coupler-rocker bearing was investigated. During the experiments, the applied load on rocker was kept constant at 410 N and the same lubricant grade was used i.e. SAE30. Fig. 13 shows the variation in temperature of C-R bearing with time due to the change in crank speed. It is evident that as the crank angular speed increases, the heat generation rate also increases due to the increase in frictional forces between contacting surfaces of the ball bearing. As a result, the temperature of C-R bearing rises.

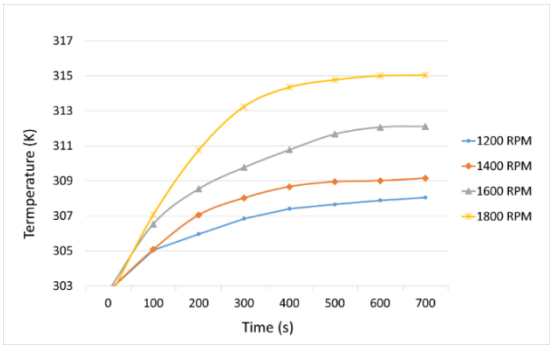

Figure 13. Crank RPM variation effect on bearing temperature

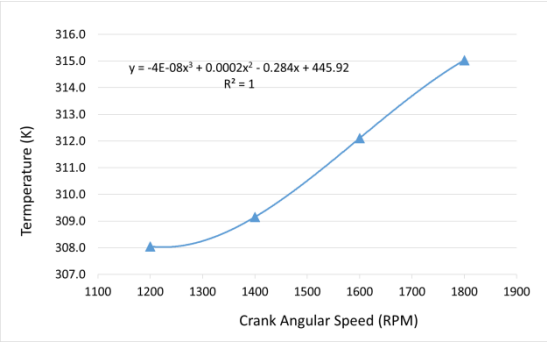

Figure 14. Trend of steady-state temperature with crank speed

The rate of increase in temperature with time is great in the beginning, but it is reduced gradually with time. The steady-state temperature for the bearing at 1200 rpm crank speed was about 308 K which was attained at around 650 s or 10.83 min. The bearing at 1400 rpm crank speed attained its steady-state temperature i.e. 309 K at around 550 s or 9.17 min. The steady-state temperature for the bearing at 1600 rpm crank speed was about 312 K which was attained at around 700 s or 11.67 min. The steady-state temperature for the bearing at 1800 rpm crank speed was about 315 K which was attained at around 600 s or 10 min. The trend of steady-state temperature values versus crank RPM is shown in fig. 14. It is observed that the trend of steady-state temperature is linear at high crank angular speeds from 1400 rpm to 1800 rpm but at speed below 1400 rpm, the steady-state temperature is higher than expected. This phenomenon is due to the high-increasing contacting and viscous friction between the bearing parts at low speeds. At high-speeds, the friction becomes constant and therefore, the steady-state temperature trend is linear. The Coefficient of Determination (R^2) for the linear curve fit was found to be exactly 1.

5.4. Effects of Oil Viscosity Grade

The effect of lubricant oil viscosity on the heat generation rate in the coupler-rocker bearing was investigated. During the experiments, the crank angular speed and applied load on rocker were kept constant i.e. 1400 rpm and 410 N respectively. Fig. 15 shows the variation in temperature of C-R bearing with time due to change in oil viscosity. It is evident that as the oil viscosity increases, the frictional moment due to viscous forces increases. This is because the thick oil film between the contacting surfaces of the C-R bearing resists the motion and thus friction increases and therefore, the heat generation rate increases. As a result of which, the temperature of C-R bearing rises. From the figure, it can be seen that all the three lubricants i.e. SAE30, SAE40 and SAE50 have almost the same effect on the C-R bearing temperature rise. Even though the difference is very small, the experimental results show that the steady-state temperature of the C-R bearing increases with the increase in lubricant viscosity.

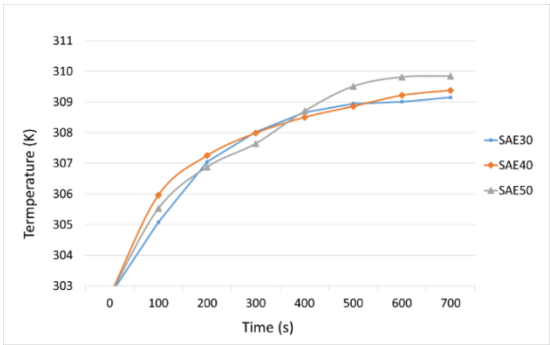

Figure 15. Lubricant viscosity variation effect on bearing temperature

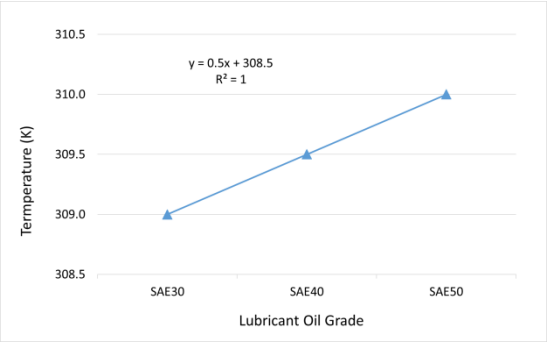

Figure 16. Trend of steady-state temperature with viscosity of oil

The rate of temperature rise is high in the beginning but then decreases with time for all cases. The test bearings lubricated with three different grade oils attained almost the same steady-state temperature at the same time. The steady-state temperatures for the test bearing lubricated by SAE30, SAE40 & SAE50 are 309 K, 309.5 K & 310 K respectively. The trend of steady-state temperature values versus lubricant oil grade is shown in fig. 16. It is observed that the trend is linear, and the steady-state temperature of the oscillating ball bearing rises linearly with the increase in lubricant oil grade. The linear behaviour of the steady-state temperature is because of the linear increase in oil viscosity grade. The Coefficient of Determination (R^2) for the linear curve fit was found to be exactly 1.

6. Conclusion

Mathematical modeling was done to calculate the heat generated in the oscillating bearing in MATLAB®. As the oil viscosity decreases with the increase in temperature, the heat generation rate decreases and becomes steady after some time. Based on this modeling, a thermal resistance network was used to predict temperatures at each node transiently of the bearing system.

Experiments were performed on the testing rig with different operating parameters. In the first set of experiments, load was varied while the crank rpm was kept constant and the oil grade was maintained. It was found that with the increase in applied load on the rocker, the bearing temperature increases owing to the increase in frictional moment due to applied load. In the second set of experiments, the crank speed was varied while the load was kept constant and the oil grade was maintained. It was found that with the increase in the crank rpm, the temperature of bearing increases due to the increase in frictional contact rate. The faster the bearing components move; the more heat is generated due to the increase in friction and thus the bearing temperature rises. In the third set of experiments, oil grade was varied while the crank rpm and load were kept constant. It was found that as the viscosity increases, the more drag is experienced by the bearing and heat dissipation reduced, and therefore the bearing temperature increased. The mathematical model and experimental results are found to be in good agreement with each other. It can be said that the thermal characteristics of the oscillating ball bearing is similar to that of the bearing performing full rotation.

Acknowledgment

The authors would like to thank Engineering, Prototyping and Innovation Centre (EPIC) for the fabrication of testing rig and Centre for Automotive Research and Electric Mobility (CAREM) for the experimental testing work station. The authors would also like to thank Yayasan Universiti Teknologi PETRONAS (YUTP) grant number 0153AA-E50 to fund this project for the Prototype Optimization of Crank-Rocker Engine.

Nomenclature

F	-force, [N]	T	-temperature, [K]
r	-spring rate, [N/mm]	A	-area, [mm^2]
x	-spring extension, [mm]	m	-mass, [kg]
M	-moment/torque, [Nmm]		
Q_f	-total frictional heat generation, [W]	*Greek Symbols*	
n	-number of revolutions, [rpm]	v	-kinematic viscosity, [mm^2/s]
k	-thermal conductivity, [W/mK]	α	-angular acceleration, [rad/s^2]
h	-heat transfer coefficient, [W/m^2K]		

References

[1] Salah E. M., Baharom. M., and Rashid A., Performance and combustion characteristics of a novel crank-rocker engine. *J. Mech. Sci. Technol*, *31*, (2017), 7, pp. 3563–3571.

[2] Jin, C., Wu, B. and Hu, Y., Heat generation modeling of ball bearing based on internal load distribution. *Tribol. Int*, *45*, (2012), 1, pp. 8–15.

[3] Choi, J. K. and Lee, D. G., Thermal Characteristics of a spindle bearing system with a gear located on the bearing span. *Int. J. Mach. Tools Manuf*, *38*, (1998), 9, pp. 1017–1030.

[4] Jeng, Y. R. and Gao, C. C., Investigation of the ball-bearing temperature rise under an oil-air lubrication system. *Proc. Inst. Mech. Eng. Part J J. Eng. Tribol*, *215*, (2001), 2, pp. 139–148.

[5] Takabi, J. and Khonsari, M. M., Experimental testing and thermal analysis of ball bearings. *Tribol. Int*, *60*, (2013), pp. 93–103.

[6] Min, X., Shuyun, J. and Ying, C., An improved thermal model for machine tool bearings. *Int. J. Mach. Tools Manuf*, *47*, (2007), 1, pp. 53–62.

[7] Immovilli, F. and Cocconcelli, M., Experimental Investigation of Shaft Radial Load Effect on Bearing Fault Signatures Detection. *IEEE Trans. Ind. Appl*, *53*, (2017), 3, pp. 2721–2729.

[8] Mizuta, K., Inoue, T., Takahashi, Y., Huang, S., Ueda, K. and Omokawa, H., Heat transfer characteristics between inner and outer rings of an angular ball bearing. *Heat Transf. - Asian Res*, *32*, (2003), 1, pp. 42–57.

[9] Khonsari, M. M., Jang, J. Y. and Fillon, M., On the Generalization of Thermohydrodynamic Analyses for Journal Bearings. *J. Tribol*, *118*, (1996), 3, pp. 571–579.

[10] Khonsari, M. M., A Review of Thermal Effects in Hydrodynamic Bearings. Part II : Journal Bearings. *A S L E Trans*, *30*, (2008), 1, pp. 26–33.

[11] Babu, S. R. and Dhamotharan, S., Simulation of Temperature Distributions of CNC Lathe Headstock Assembly. *Int. J. Mech. Mechatronics Eng*, *14*, (2014), 6, pp. 99–103.

[12] Qi, L., Zhang, G. and Liu, Y., Modeling and simulation of the thermal network in a space gear-bearing system. *2010 IEEE Int. Conf. Inf. Autom. ICIA*, (2010), pp. 201–205.

[13] Wang, L. Q., Chen, G. C., Gu, L and Zheng, D. Z., Operating temperature in high-speed ball bearing. *Proc. Inst. Mech. Eng. Part C J. Mech. Eng. Sci, 221,* (2007), 3, pp. 353–359.

[14] Moorthy, R. S. and Raja, V. P., An Improved Analytical Model for Prediction of Heat Generation in Angular Contact Ball Bearing. *Arab. J. Sci. Eng, 39,* (2014), 11, pp. 8111–8119.

[15] Winer, W. O., Bair, S. and Gecim, B., Thermal resistance of a tapered roller bearing. *ASLE Trans, 29*, (1986), 4, pp. 539–547.

[16] Pouly, F., Changenet, C., Ville, F., Velex, P. and Damiens, B., Power loss predictions in high-speed rolling element bearings using thermal networks. *Tribol. Trans, 53,* (2010), 6, pp. 957–967.

[17] Pouly, F., Changenet, C., Ville, F., Velex, P. and Damiens, B., Investigations on the power losses and thermal behaviour of rolling element bearings. *Proc. Inst. Mech. Eng. Part J J. Eng. Tribol, 224*, (2010), 9, pp. 925–933.

[18] Jorgensen, B. R. and Shin, Y. C., Dynamics of Machine Tool Spindle/Bearing Systems Under Thermal Growth. *J. Tribol, 119,* (1997), 4, pp. 875.

[19] Harris, T. A. and Kotzalas, M. N., *Rolling Bearing Analysis*, revised 5th ed. Taylor & Francis, (2006).

[20] Jamil. A., Baharom. M. B., and Lemma. T. A., Mathematical Modelling and Transient Thermal Analysis of Coupler-Rocker Bearing. *MATEC Web Conf, 225,* (2018).

[21] Stein, J. L. and Tu, J. F., A State-Space Model for Monitoring Thermally Induced Preload in Anti-Friction Spindle Bearings of High-Speed Machine Tools. *J. Dyn. Syst. Meas. Control, 116,* (1994), 3, pp. 372–386.

[22] Bejan. A., *Convection Heat Transfer*, 4th ed. John Wiley & Sons, (2013).

[23] Jang, J. Y., Khonsari, M. M. and Pascovici, M. D., Modeling aspects of a rate-controlled seizure in an unloaded journal bearing. *Tribol. Trans, 41,* (1998), 4, pp. 481–488.

[24] Khonsari, M. M. and Booser, E. R., *Applied Tribology: Bearing Design and Lubrication*, 3rd ed. John Wiley & Sons, (2017).